

A New Perfluorinated F₂₁-Tp Scorpionate Ligand: Enhanced Alkane Functionalization by Carbene Insertion with (F₂₁-Tp)M Catalysts (M = Cu, Ag)

Emmanuelle Despagnet-Ayoub,[†] Kane Jacob,[†] Laure Vendier,[†] Michel Etienne,^{*,†} Eleuterio Álvarez,[§] Ana Caballero,[‡] M. Mar Díaz-Requejo,^{*,‡} and Pedro J. Pérez^{*,‡}

Laboratoire de Chimie de Coordination du CNRS, UPR 8241 Liée par Conventions à l'Université Paul Sabatier et à l'Institut National Polytechnique de Toulouse, 205 Route de Narbonne, 31077 Toulouse Cedex 4, France, Instituto de Investigaciones Químicas, CSIC-Universidad de Sevilla, Avenida Américo Vespucio 49, 41092 Sevilla, Spain, and Laboratorio de Catálisis Homogénea, Departamento de Química y Ciencia de los Materiales, Unidad Asociada al CSIC, Campus de El Carmen s/n, Universidad de Huelva, 21007-Huelva, Spain

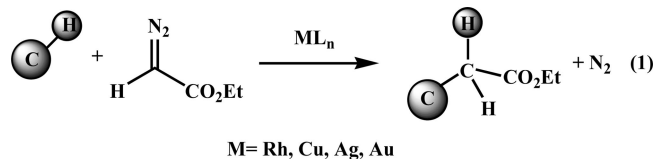
Received June 8, 2008

The new tris(indazolyl)borate ligand [F₂₁-Tp^{4Bo,3CF3}]Tl (**1**) has been prepared and structurally characterized. The reaction of its thallium salt with copper iodide or silver triflate afforded the complexes [F₂₁-Tp^{4Bo,3CF3}]ML (M = Cu, L = NCMe, **2**; M = Ag, L = Me₂CO, **4**), from which the carbonyl adducts [F₂₁-Tp^{4Bo,3CF3}]M(CO) (M = Cu, **3**; M = Ag, **5**) have also been obtained. Complexes **2**–**5** have been characterized by spectroscopic and X-ray studies, from which the existence of electron-deficient metal centers could be envisaged. Complexes **2** and **4** have been employed as catalysts for the reaction of alkanes and cycloalkanes with ethyl diazoacetate. The silver complex displays excellent catalytic activity for the insertion of the carbene into the alkane CH bonds. Functionalized products are obtained in high yield (>90%) with low catalyst loadings (0.5%). TON values of 200 have been reached, 10 times higher than any other group 11 metal-based catalyst already reported for this transformation.

Introduction

The catalytic conversion of plain hydrocarbons such as alkanes into functionalized molecules is of enormous interest given the availability of such raw materials.^{1,2} One of the yet underdeveloped methodologies to accomplish such a goal is the insertion of carbene units, in situ generated from metal-mediated decomposition of diazo compounds, into the C–H bond of the alkane (eq 1).^{3,4} Rhodium-based catalysts were reported in the early 1980s to promote this transformation, with moderate to high yield and TON values of ca. 1000.⁵ In the past decade, coinage metal-based catalysts have been reported for this

transformation, although their activities are yet below those of rhodium catalysts.⁶ Tris(pyrazolyl)borate complexes of copper⁷ and silver^{8,9} have been employed for the insertion of CHCO₂Et groups (from ethyl diazoacetate, EDA, N₂CHCO₂Et) into the C–H bonds of linear or branched alkanes: the best results have been achieved with the Tp^{Br3} or Tp^{(CF₃)₂} derivatives, and silver



as the metal (Scheme 1).^{8,9} Another family of catalysts with NHC ligands (NHC = N-heterocyclic carbene) has been reported for alkane functionalization with Cu or Au (Scheme 1).¹⁰ Overall, all these catalysts promote the formal insertion of the carbene group CHCO₂Et into primary, secondary, or tertiary C–H bonds of simple alkanes such as hexane or 2-methylbutane, among others. However, there are two common

* Corresponding authors. E-mail: etienne@lcc-toulouse.fr; mmdiaz@dqcm.uhu.es; perez@dqcm.uhu.es.

[†] CNRS-Université Paul Sabatier.

[§] CSIC-Universidad de Sevilla.

[‡] Universidad de Huelva.

(1) (a) Shilov, A. E.; Shul'pin, G. B. *Activation and Catalytic Reactions of Saturated Hydrocarbons in the Presence of Metal Complexes*; Kluwer: Dordrecht 2000. (b) Davies, J. A.; Watson, P. L.; Liebman, J. F.; Greenberg, A. *Selective Hydrocarbon Activation, Principles and Progress*; VCH Publishers: New York, 1990. (c) Shilov, A. E.; Shul'pin, G. B. *Chem. Rev.* **1997**, *97*, 2879. (d) Arndtsen, B. A.; Bergman, R. G.; Mobleyand, T. A.; Peterson, T. H. *Acc. Chem. Res.* **1995**, *28*, 154.

(2) (a) Bergman, R. G. *Nature* **2007**, *446*, 391. (b) Labinger, J. A.; Bercaw, J. E. *Nature* **2002**, *417*, 507.

(3) (a) Doyle, M. P.; McKervey, M. A.; Ye, T. *Modern Catalytic Methods for Organic Synthesis with Diazo Compounds*; John Wiley & Sons: New York, 1998.

(4) (a) Davies, H. M. L. *Nature* **2008**, *451*, 417. (b) Davies, H. M. L.; Beckwith, R. E. J. *Chem. Rev.* **2003**, *103*, 2861. For specific work of asymmetric induction with alkanes see: (c) Davies, H. M. L.; Hansen, T. *J. Am. Chem. Soc.* **1997**, *119*, 9075. (d) Davies, H. M. L.; Hansen, T.; Churchill, M. R. *J. Am. Chem. Soc.* **2000**, *122*, 3063.

(5) (a) Demonceau, A.; Noels, A. F.; Hubert, A.; Teyssié, P. *J. Chem. Soc., Chem. Commun.* **1981**, 688. (b) Callot, H. J.; Metz, F. *Nouv. J. Chim.* **1985**, *9*, 167. (c) Endres, A.; Maas, G. *J. Organomet. Chem.* **2002**, *643*, 174.

(6) Díaz-Requejo, M. M.; Belderrain, T. R.; Nicasio, M. C.; Pérez, P. J. *Dalton Trans.* **2006**, 5559.

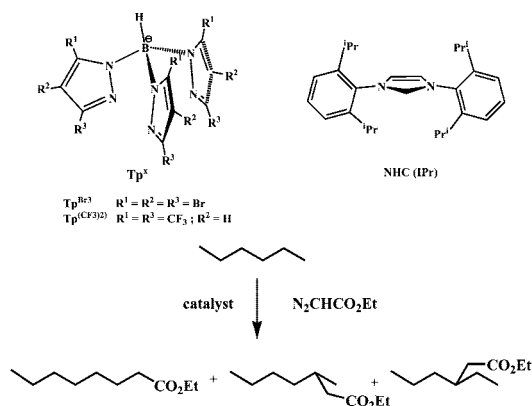
(7) (a) Díaz-Requejo, M. M.; Belderrain, T. R.; Nicasio, M. C.; Trofimenko, S.; Pérez, P. J. *J. Am. Chem. Soc.* **2002**, *124*, 896. (b) Caballero, A.; Díaz-Requejo, M. M.; Belderrain, T. R.; Nicasio, M. C.; Trofimenko, S.; Pérez, P. J. *J. Am. Chem. Soc.* **2003**, *125*, 1446. (c) Caballero, A.; Díaz-Requejo, M. M.; Belderrain, T. R.; Nicasio, M. C.; Trofimenko, S.; Pérez, P. J. *Organometallics* **2003**, *22*, 4145.

(8) (a) Dias, H. V. R.; Browning, R. G.; Richey, S. A.; Lovely, C. J. *Organometallics* **2004**, *23*, 1200. (b) Dias, H. V. R.; Browning, R. G.; Richey, S. A.; Lovely, C. J. *Organometallics* **2005**, *24*, 5784.

(9) Urbano, J.; Belderrain, T. R.; Nicasio, M. C.; Trofimenko, S.; Díaz-Requejo, M. M.; Pérez, P. J. *Organometallics* **2005**, *24*, 1528.

(10) Frutos, M. R.; Frémont, P. de; Nolan, S. P.; Díaz-Requejo, M. M.; Pérez, P. J. *Organometallics* **2006**, *25*, 2237.

Scheme 1. Synthesis of the Copper Complexes 2 and 3



Catalyst	Catalyst loading ^a	TON ^b	reference
$Rh_2(OOCCF_3)_4$	0.06%	1500	5a
RhTPPI	0.1%	1000	5b
$Rh_2(OOCCF_3)_4$ ^c	1%	100	5c
$Tp^{Br^3}Cu(NCMe)$	5%	20	7b
$[Tp^{Br^3}Ag]_2$	5%	20	9
$Tp^{(CF_3)_2}Cu(thf)$	5%	20	8
$Tp^{(CF_3)_2}Ag(thf)$	5%	20	8
$IPrCu(NCMe)BF_4$	5%	20	10
$IPrAu(NCMe)BF_4$	5%	20	10

^aPercentage referred to EDA. ^bAs mmol EDA converted by mmol catalyst. ^cMethyl diazoacetate as the carbene source

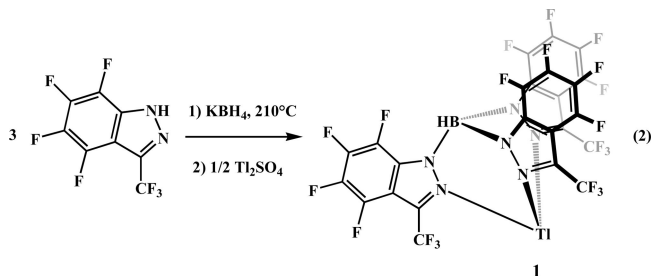
main drawbacks for these group 11 metal-based catalysts: (a) rather high catalyst loadings, ca. 5%, compared to those of the best rhodium catalyst (<1%), and (b) quite low turnover numbers, in the range 20–40 (as mmol diazoacetate consumed by mmol catalyst). On that basis, we decided to design a new catalyst based on coinage metals that could surpass those drawbacks, therefore decreasing catalyst loadings and improving TON values.

As mentioned above, good catalytic results were obtained with Tp^xAg derivatives where $Tp^x = Tp^{Br^3}$ or $Tp^{(CF_3)_2}$. Therefore, we thought that a perfluorinated ligand would contain the properties of the perbromo Tp^{Br^3} (devoid of CH bonds) and the fluorinated $Tp^{(CF_3)_2}$ (with 18 F on it). To the best of our knowledge, there are no reports on the use of a perfluorinated ligand in this kind of transformations.⁶ In this contribution we report the synthesis of the new perfluorinated homoscorpionate ligand hydrotris(3-trifluoromethyl-4,5,6,7-tetrafluoroindazolyl)borate, $F_{21}Tp^{4Bo,3CF_3}$, the synthesis of its copper and silver complexes of composition $[F_{21}Tp^{4Bo,3CF_3}]ML$ ($M = Cu, Ag$; $L = NCMe, CO$), and the catalytic activity of such complexes toward the functionalization of alkanes with ethyl diazoacetate. The catalytic results have shown that those complexes display a remarkable activity that clearly improves those reported to date with any other coinage metal-based catalyst.

Results and Discussion

A New Indazolylborate Ligand. The new perfluorinated hydrotris(3-trifluoromethyl-4,5,6,7-tetrafluoroindazolyl)borate salt $Tl[F_{21}Tp^{4Bo,3CF_3}]$ (**1**) was obtained in ca. 27% yield upon heating 3.5 equiv of 3-trifluoromethyl-4,5,6,7-tetrafluoroinda-

zole¹¹ with potassium borohydride followed by cation exchange with thallium sulfate and then crystallization (eq 2). Full characterization includes correct elemental (C, H, N) analysis, IR ($\nu(BH) = 2449\text{ cm}^{-1}$), and ¹⁹F, ¹³C, and ¹¹B NMR data as well as the determination of an X-ray crystal structure.



The X-ray structure of **1** is shown in Figure 1. There are two independent molecules of **1** in the asymmetric unit, almost parallel to each other (5.3° between indazolyl planes containing N1 and N7) with the $B \cdots Tl$ vectors roughly oriented along the cell parameter a . Up to seven $C-F \cdots C$ (aromatic) close contacts in the range 2.99–3.13 Å (3.07 Å average) with a $C-F \cdots$ aromatic plane angle of ca. 46° are present between the two units, suggesting possible interactions.¹² Similar interactions link the asymmetric units together. An additional intermolecular close contact exists between Tl(1) and F(41) that amounts to 3.37 Å, and Tl(1) is also 3.23 Å away from another fluorine, F(35), belonging to the next translated unit. These contacts are certainly loose (intramolecular $Tl(1) \cdots F$ contacts are in the range 2.98–3.22 Å and $Tl(2) \cdots F$ are in the range 3.07–3.13 Å, the difference being principally attributable to slightly different conformations of the CF_3 groups), but may contribute to the overall orientation and the slight but noticeable difference between the two molecules in the asymmetric unit. In both molecules, the thallium has a pyramidal geometry with equal $Tl-N$ bond lengths of 2.61 Å and $N-Tl-N$ angles in the range $68.8(2)–71.1(2)^\circ$. The $Tl-N$ bonds are shorter and the $N-Tl-N$ angles are slightly larger than those in the closely related $TlTp^{(CF_3)_2}$ ($Tl-N = 2.724(7), 2.675(10)$ Å; $N-Tl-N = 67.9(2)^\circ, 68.7(3)^\circ$).¹³ The metric parameters are not significantly different from those in most $TlTp^x$ complexes, where $Tl-N$ bond lengths are slightly shorter, around 2.57 Å, and $N-Tl-N$ angles slightly larger, around $72–79^\circ$. The conformation of all CF_3 groups in **1** is such that a $C-F$ bond eclipses a $C-N$ bond, thereby directing this fluorine toward the thallium atom. The other two fluorines of any given CF_3 group are then staggered with respect to the benzo ring. This is a notable difference with $TlTp^{(CF_3)_2}$, in which the conformation of the CF_3 groups is reversed, a $C-F$ bond eclipsing a $C-C$ bond of pyrazole.¹³ A key structural parameter of scorpionate ligands is their cone angle.¹⁴ That estimated for **1** with the innermost fluorines is 243° for the most regular molecule containing Tl(2), slightly larger than those for $TlTp^{(CF_3)_2}$ (237°), for the 3-methylindazolylborate salt $TlTp^{4Bo,3Me}$ (235°), and for $TlTp^{Me2}$ (239°).¹⁴

(11) Teichert, J.; Oulié, P.; Jacob, K.; Vendier, L.; Etienne, M.; Claramunt, R. M.; López, C.; Medina, C. P.; Alkorta, I.; Elguero, J. *New J. Chem.* **2007**, *31*, 936.

(12) (a) Reichenbacher, K.; Süß, H. I.; Hulliger, J. *Chem. Soc. Rev.* **2005**, *34*, 22. (b) Hunter, C. A.; Lawson, K. R.; Perkins, J.; Urch, C. J. *J. Chem. Soc., Perkin Trans. 2* **2001**, 651.

(13) Renn, O.; Venanzi, L. M.; Martelletti, A.; Gramlich, V. *Helv. Chim. Acta* **1995**, *78*, 993.

(14) Trofimenko, S. *Scorpionates: The Coordination Chemistry of Polypyrazolylborate Ligands*; Imperial College Press: London, 1999.

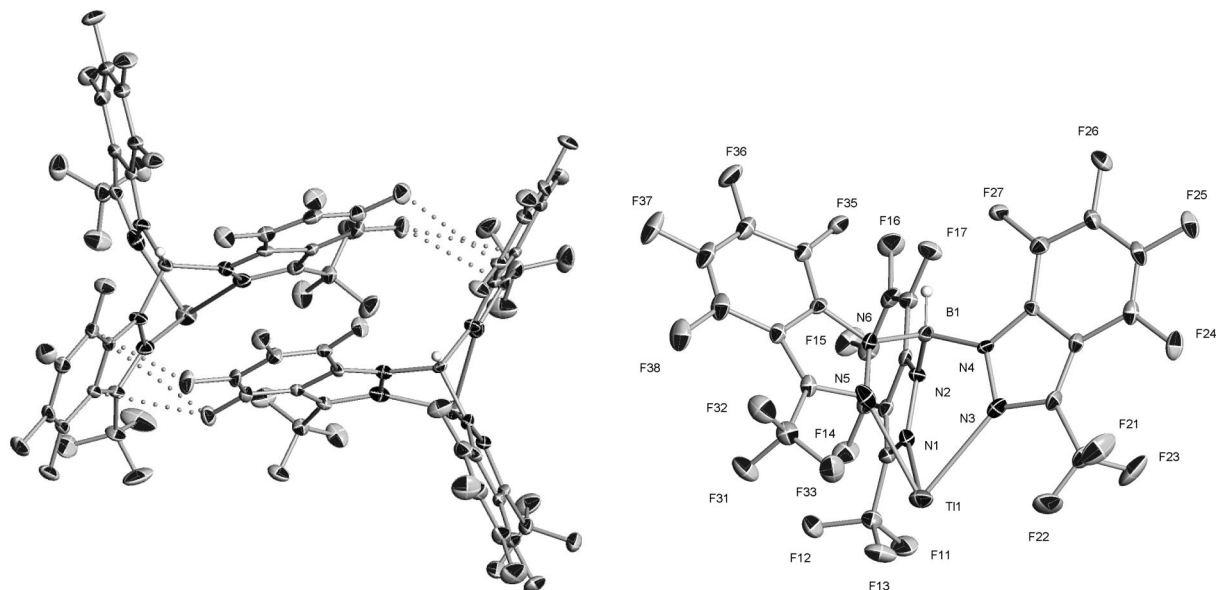
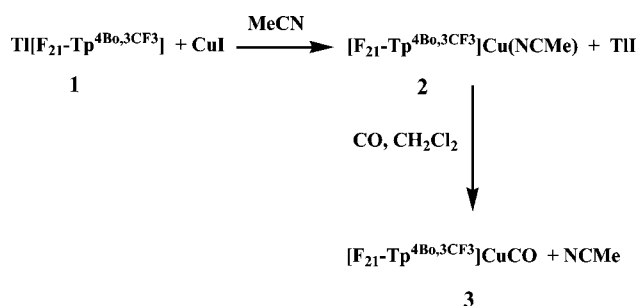


Figure 1. X-ray structure of **1**. Plot of the asymmetric unit with intermolecular CF...aromatic and TI...F short contacts (left), also a weak intermolecular π - π stacking interactions through the phenyl rings of pyrazolyl groups (3.84–3.95 Å), and ORTEP plot of one independent molecule with thermal ellipsoids at the 50% probability level (right).

Table 1. Carbonyl Stretching Frequencies and Selected Bond Distances of Copper(I) and Silver(I) Carbonyl Complexes

	ν_{CO} (cm^{-1})	M–C (Å)	M–N (av) (Å)	C–O (Å)	ref
Tp ^{iPr} 2CuCO	2056	1.769(8)	2.018(4)	1.118(10)	1
TpCuCO	2083	1.755(11)	2.048(4)	1.120(13)	18
Tp ^{CF3} CuCO	2100	1.790(4)	2.052(3)	1.126(5)	19a
Tp ^{Br3} CuCO	2110				7c
[F ₂₁ -Tp ^{4Bo,3CF3} Cu(CO) (3)	2132	1.807(4)	2.093(11)	1.130(5)	this work
Tp ^{(CF3)2} CuCO	2137	1.808(4)	2.052(15)	1.110(5)	19b
CO	2143			1.1283	20
Tp ^{C2F5} AgCO	2153	2.030(4)	2.314(15)	1.117(4)	19c
Tp ^{Br3} AgCO	2157				9
[F ₂₁ -Tp ^{4Bo,3CF3}]Ag(CO) (5)	2167	2.027(3)	2.318(5)	1.073(4)	this work
Tp ^{(CF3)2} AgCO	2178	2.037(5)	2.328(28)	1.116(7)	15

Scheme 2



Synthesis and Characterization of Copper(I) Complexes. The hydrotris(3-trifluoromethyl-4,5,6,7-tetrafluoroindazolyl)borate copper(I) complex [F₂₁-Tp^{4Bo,3CF₃}]₃Cu(CH₃CN) (**2**) was synthesized by addition of copper(I) iodide to a solution of the thallium salt TI[F₂₁-Tp^{4Bo,3CF₃}] (**1**) in acetonitrile (Scheme 2) and isolated as a white powder in 88% yield after workup. Only one type of indazolyl ring is observed by NMR, indicating C_{3v} symmetry, and chemical shifts and coupling constants for the indazolylborate ligand are similar to those for **1**. Bubbling of CO throughout CH₂Cl₂ solutions of **2** yields the carbonyl adduct [F₂₁-Tp^{4Bo,3CF₃}]₃Cu(CO) (**3**), as inferred from the observation of an absorption at 2126 cm⁻¹, which moves to 2132 cm⁻¹ in the solid state, corresponding to $\nu(\text{CO})$. Complex **3** readily loses CO under reduced pressure (although a correct elemental analysis for **3** was successfully obtained), and weakly coordinat-

ing solvents such as dichloromethane and chloroform should be used to avoid the displacement of CO. This particularly high value of $\nu(\text{CO})$ is in the same range as that for Tp^{(CF₃)₂}Cu(CO)¹⁵ and is very close to the value observed for free CO (2143 cm⁻¹) (see Table 1). In the ¹³C{¹H} NMR spectrum, the carbonyl carbon is detected at δ 172, in a typical range for copper carbonyl complexes [Tp^{Ph₂}Cu(CO): δ 173.8; Tp^{iBu,iPr}Cu(CO): δ 174.0].¹⁶ This value is upfield from that of free CO (δ 184) and those for classical metal carbonyl complexes where metal-to-CO π -back-bonding is significant (184 < δ < 223).¹⁷ According to the IR and NMR data, there is very poor π -back-donation from the copper to the carbonyl in **3**, the CO ligand mainly acting as a σ -donor.

Complexes **2** and **3** were characterized on the basis of their analytical and spectroscopic data. The equivalence of the three pyrazolyl rings indicated the existence of a C_{3v} symmetry in solution, in accord with the geometries shown in Figure 2. In order to unambiguously determine the structures in the solid state, X-ray studies were carried out with both complexes, the structures being shown in Figure 2. The acetonitrile adduct displays geometrical parameters similar to other known Tp^x-Cu(NCMe) (Tp^x = Tp^{Ms}, Tp^{(CF₃)₂}), including the usually

(15) Dias, H. V. R.; Wang, Z.; Jin, W. *Inorg. Chem.* **1997**, *36*, 6205.

(16) Fujisawa, K.; Ono, T.; Ishikawa, Y.; Amir, N.; Miyashita, Y.; Okamoto, K.; Lehnert, N. *Inorg. Chem.* **2006**, *45*, 1698.

(17) Weber, L. *Angew. Chem., Int. Ed. Engl.* **1994**, *33*, 1077.

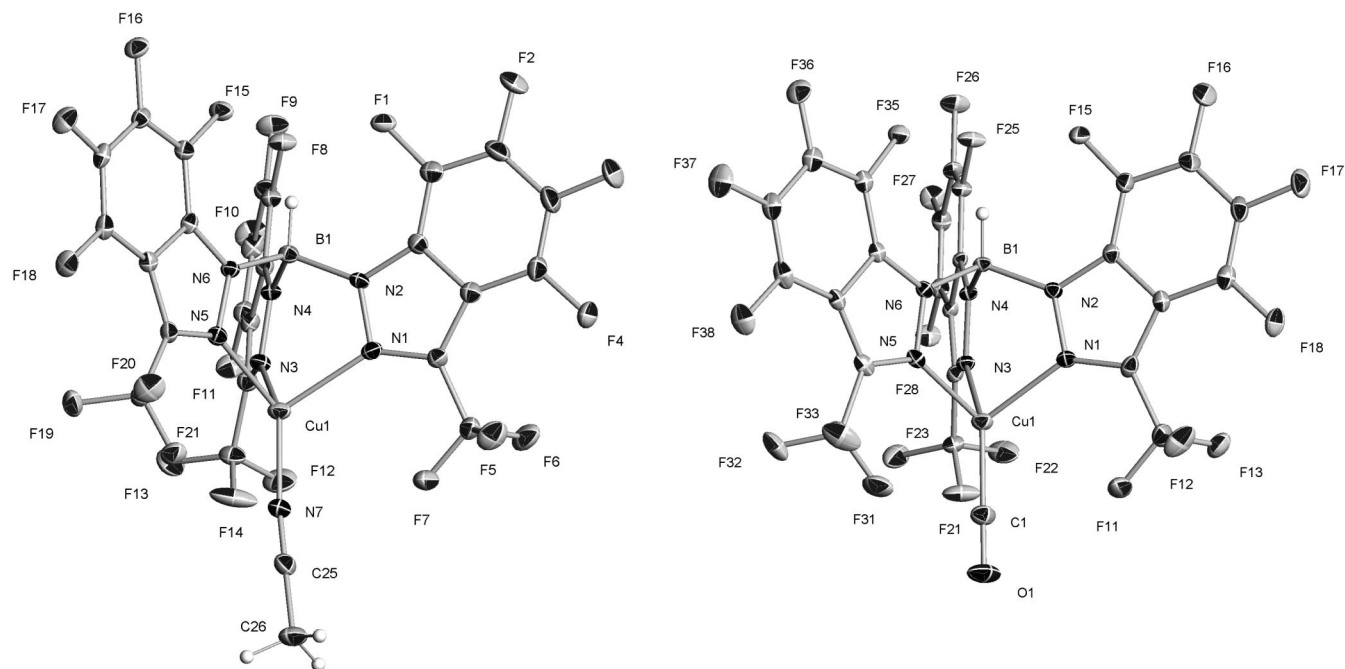
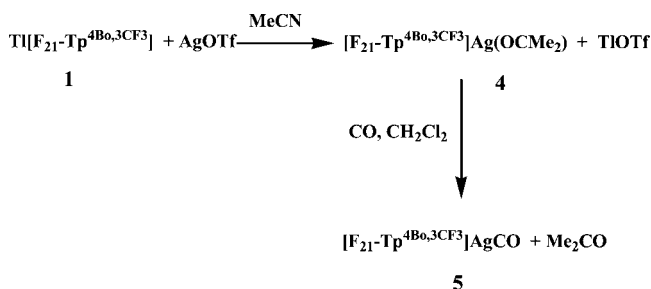


Figure 2. Molecular structures of complexes **2** (left) and **3** (right). Selected bond distances (Å) and angles for **2** (deg): Cu(1)–N(7) 1.8988(18), Cu(1)–N(1) 2.118(2), Cu(1)–N(3) 2.0870(18), Cu(1)–N(5) 2.1013(19), C(25)–N(7)–Cu(1) 171.7(2). For **3**: Cu(1)–C(1) 1.807(4), Cu(1)–N(1) 2.095(3), Cu(1)–N(3) 2.106(3), Cu(1)–N(5) 2.079(3), C(1)–O(1) 1.130(5); O(1)–C(1)–Cu(1) 177.9(4). Thermal ellipsoids are drawn at the 50% probability level.

Scheme 3. Synthesis of the Silver Complexes **4** and **5**



observed deviation of the acetonitrile ligand from the ideal location along the B–Cu axis.

Crystals of **3** were obtained from a dichloromethane/pentane solution at -25°C under a CO atmosphere. The copper center (Figure 2) adopts a distorted tetrahedral coordination, the Cu–C–O moiety being essentially linear (Cu–C–O: $177.9(4)^\circ$). Complex **3** has roughly C_{3v} symmetry with mirror planes containing the B–H, one indazolyl ring, the copper center, and the CO unit. The B–N bond lengths (1.544(5), 1.550(5), and 1.551(5) Å) are in the typical range for a borate ligand. The interesting features in the structure of **3** concern the relatively long Cu–C (1.807(4) Å) and Cu–N (2.093(11) Å) bond distances, fully comparable to those for other fluorinated tris(pyrazolyl)borate copper carbonyl complexes (Table 1). These results are consistent with poor π -back-donation from the copper to the carbonyl, in line with the IR data.

Synthesis and Characterization of Silver(I) Complexes. The white hydrotris(3-trifluoromethyl-4,5,6,7-tetrafluoroindazolyl)borate silver(I) acetone complex $[\text{F}_{21}\text{-Tp}^{4\text{Bo},3\text{CF}_3}]\text{Ag}(\text{CH}_3\text{COCH}_3)$ (**4**) was prepared in 73% yield by mixing silver(I) triflate and **1** in acetone (Scheme 3). Crystals were obtained by cooling a dichloromethane/pentane solution of **4** at -25°C or by slow evaporation of an acetone solution, and an X-ray study was carried out. Unfortunately, the molecular

structure of **4** is severely disordered around the acetone fragment (see Supporting Information for an ORTEP view).

The synthesis of the silver(I) carbonyl complex $[\text{F}_{21}\text{-Tp}^{4\text{Bo},3\text{CF}_3}]\text{Ag}(\text{CO})$ (**5**) was accomplished by bubbling CO gas through a solution of **4** in dichloromethane for 2 h (Scheme 3). As for the copper analogue, complex **5** readily loses CO under reduced pressure or in the presence of a coordinating solvent. In dichloromethane solution and in the solid state, this complex displays a strong $\nu(\text{CO})$ absorption centered at 2167 cm^{-1} in its IR spectrum (Table 1). This value is higher than that of free CO (2143 cm^{-1}) and is 10 cm^{-1} lower than that in $\text{Tp}^{(\text{CF}_3)_2}\text{AgCO}$. Moreover, $\nu(\text{CO})$ in **5** is higher than that in the copper analogue **3**, in agreement with decreased M→CO π -back-donation when going down the group from Cu(I) to Ag(I).^{21,22} The $^{13}\text{C}\{^1\text{H}\}$ NMR of **5** in CDCl_3 exhibits a signal at δ 178 corresponding to the CO ligand. These IR and NMR data confirm a nonclassical metal carbonyl complex, with mainly σ -type Ag–CO interaction.

Crystals of **5** were grown from a dichloromethane/pentane solution at -25°C , and the structure of **5** was determined by X-ray crystallography (Figure 3). The silver center adopts a pseudotetrahedral environment. The Ag–C–O is essentially linear ($175.9(4)^\circ$). The C–O bond distance (1.073(7) Å) is slightly short by not exceptional.²³ The Ag–CO bond length (2.027(3) Å) is within the same range as that in $\text{Tp}^{(\text{CF}_3)_2}\text{AgCO}$ (2.037(5) Å) but shorter than the corresponding M–CO bond

(18) (a) Bruce, M. I.; Ostaszewski, A. P. *J. Chem. Soc., Dalton Trans.* **1973**, 2433. (b) Churchill, M. R.; DeBoer, B. G.; Rotella, F. J.; Abu-Salah, O. M.; Bruce, M. I. *Inorg. Chem.* **1975**, *14*, 2051.

(19) (a) Dias, R. H. V.; Kim, H.-J.; Lu, H.-L.; Rajeshwar, K.; de Tacconi, N. R.; Derecskei-Kovacs, A.; Marynick, D. S. *Organometallics* **1996**, *15*, 2994. (b) Dias, R. H. V.; Lu, H.-L. *Inorg. Chem.* **1995**, *34*, 5380. (c) Dias, R. H. V.; Wang, X. *Dalton Trans.* **2005**, 2985.

(20) Braterman, P. S. *Metal Carbonyl Spectra*; Academic Press: New York, 1975; p 177.

(21) Lupinetti, A. J.; Strauss, S. H.; Frenking, G. *Prog. Inorg. Chem.* **2001**, *49*, 1.

(22) Dias, R. H. V.; Jin, W. *Inorg. Chem.* **1996**, *35*, 3687.

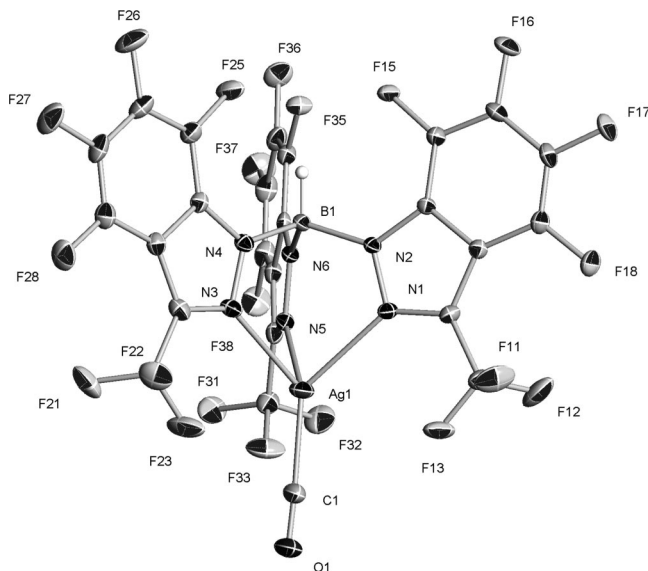


Figure 3. Molecular structure of $[F_{21}\text{-Tp}^{4\text{Bo},3\text{CF}_3}]\text{Ag}(\text{CO})$ (**5**). Selected bond distances (Å) and angles (deg): $\text{Ag}(1)\text{-C}(1)$ 2.027(3), $\text{Ag}(1)\text{-N}(1)$ 2.325(2), $\text{Ag}(1)\text{-N}(3)$ 2.313(2), $\text{Ag}(1)\text{-N}(5)$ 2.317(2), $\text{C}(1)\text{-O}(1)$ 1.073(7); $\text{O}(1)\text{-C}(1)\text{-Ag}(1)$ 175.9(4).

observed for the copper(I) complex **3** (1.807(4) Å). The same trend is observed for the Ag–N bond distances.

Catalytic Functionalization of C–H Bonds of Alkanes with Ethyl Diazoacetate. The metal-catalyzed decomposition of ethyl diazoacetate has been extensively employed for the transfer of the carbene moiety CHCO_2Et to saturated and unsaturated substrates.^{3,4} Among them, several examples, but not so many, concern the C–H bonds of alkanes.⁶ The catalytic insertion of such a carbene unit into a C–H bond usually requires an electrophilic metal center that enhances the reactivity of transient metalcarbene intermediates toward the poor nucleophile C–H bond. Therefore, the lower the electron density at the metal center, the higher the potential of that complex to act as a good catalyst for this transformation. Collected spectroscopic and structural data for complexes **2–5** have shown that the Cu and Ag derivatives containing the new ligand $[F_{21}\text{-Tp}^{4\text{Bo},3\text{CF}_3}]$ seems to be electron-deficient metal centers. On that basis, we have carried out a series of reactions in which linear or branched alkanes have been reacted with ethyl diazoacetate in the presence of complex **2** or **4** as the catalyst. A typical experiment was performed in the following manner: 0.008 mmol of the catalyst was dissolved in the alkane, and ethyl diazoacetate (EDA, 25–30 equiv with respect to catalyst) was added in one

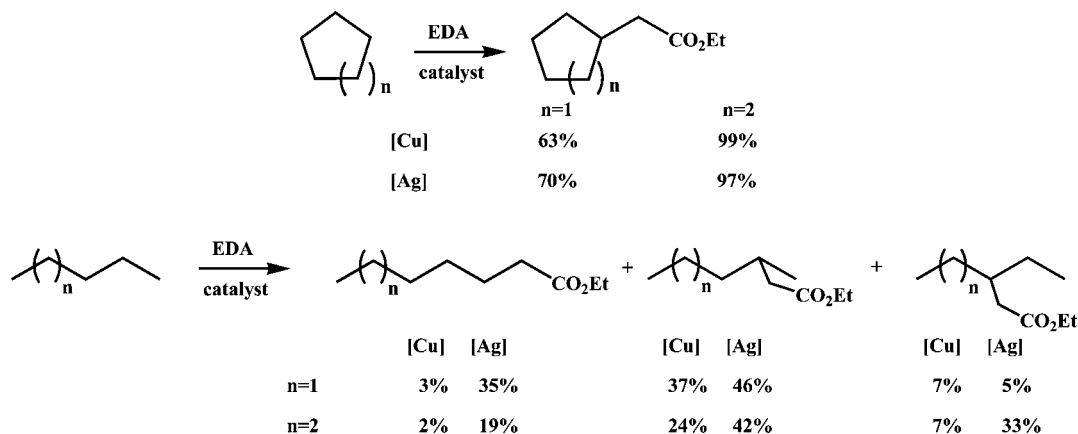
portion. The compounds are quite soluble in hydrocarbons, at variance with other coinage metal catalysts, which usually require the presence of a cosolvent. After 3 h of stirring at room temperature, the mixture was analyzed by GC, revealing that the diazo compound had been consumed. Products derived from the insertion of the carbene CHCO_2Et group into C–H bonds of the alkanes were observed. Scheme 4 displays the results obtained with C5 and C6 cycloalkanes and linear alkanes. A general trend is observed: the silver-based catalyst provides higher conversions into the functionalized products. In addition, the selectivity toward primary sites is also enhanced with the silver catalyst, the copper analogue providing nearly undetectable amounts of such products.

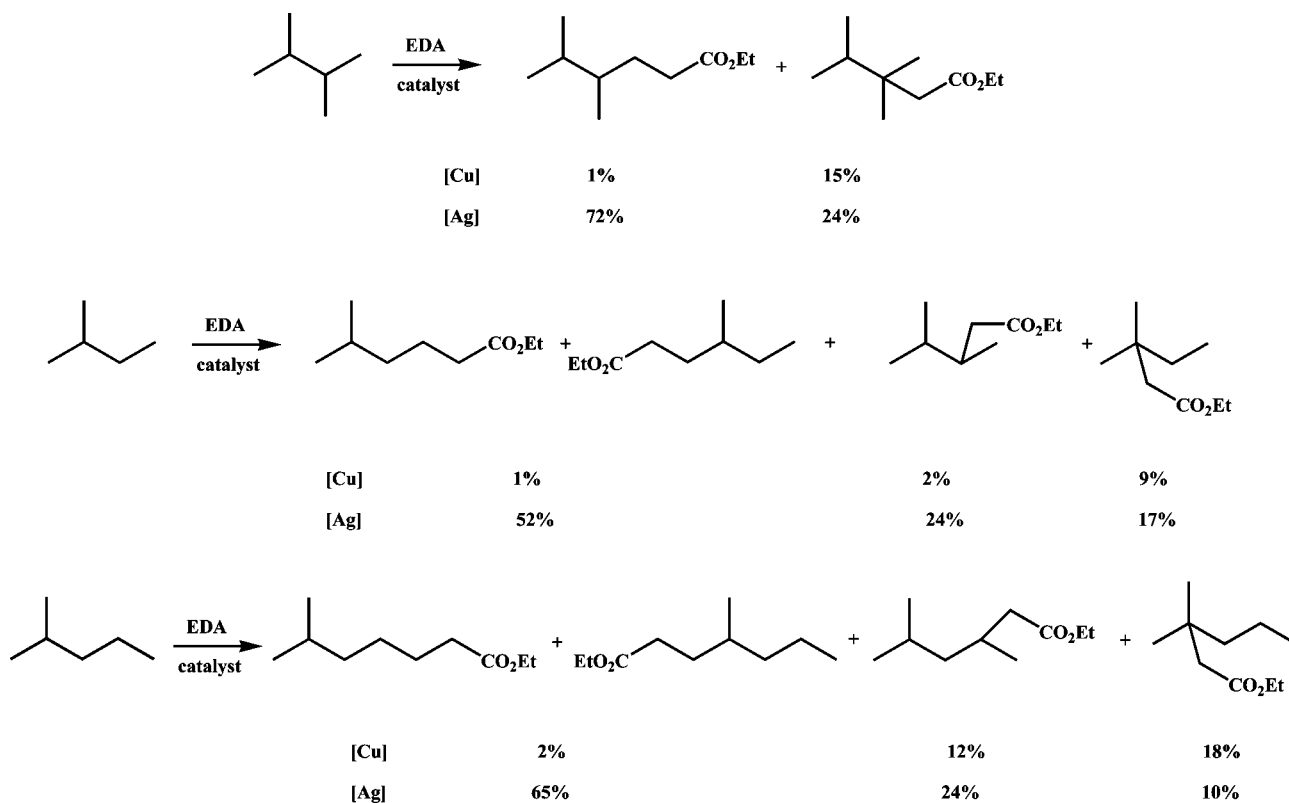
The substrates shown in Scheme 4 contain primary and/or secondary C–H bonds. A second series of experiments was carried out with branched alkanes (Scheme 5), thereby screening tertiary sites as well. Under identical conditions, the same trends about activity and selectivity toward C–H insertion still operate: the silver catalyst **4** provides higher conversions into the functionalized products as well as higher amounts of the primary site derivatives. In addition, the tertiary C–H bonds seem to be more prone to undergo the insertion reaction. In all cases, higher selectivity is found for tertiary sites. For example, with 2,3-dimethylbutane as the substrate, a 75:25 distribution of products, primary versus tertiary site functionalization, was observed. When this distribution is normalized by the number of hydrogens of each type, 12 and 2, respectively, the corrected regioselectivity is ca. 1:2 favoring the tertiary sites. This means that functionalization of the most sterically hindered, weaker C–H bonds is favored over that of primary and secondary CH bonds. These results are in good agreement with theoretical studies²⁴ that have shown that the energy barriers for this carbene insertion reaction follow the order tertiary > secondary > primary and that for a given type of C–H bond the barriers for the silver catalyst are lower than those for the copper catalyst. The latter explains the functionalization of the primary sites with silver but not with copper.

The TON values are 25 and 30 for the copper- and silver-based catalysts, respectively. These values are slightly higher than those reported for other coinage metal catalysts (Table 1). For the silver catalyst in addition, more than 90% of the EDA is converted into functionalized products, with less than 10% of the ethyl diazoacetate leading to the side coupling products diethyl fumarate and maleate: chemoselectivity is quite high, even when the diazo compound is added in one portion.

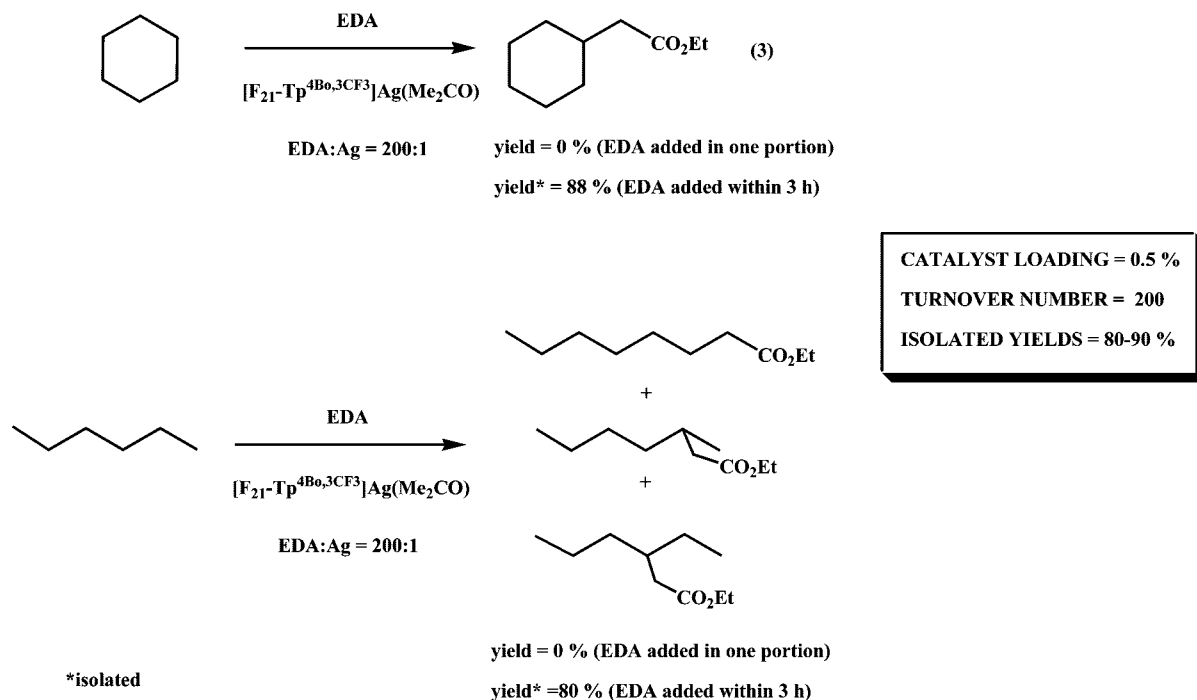
Having demonstrated that the silver complex **4** was capable of inducing the insertion of the CHCO_2Et group into the C–H

Scheme 4. Functionalization of Linear Alkanes and Cycloalkanes with Complexes **2** ([Cu]) and **4** ([Ag])



Scheme 5. Functionalization of Branched Alkanes with Complexes 2 ([Cu]) and 4 ([Ag])^a

^aPercentage corresponds to distribution of products (diethyl fumarate and maleate accounted for 100% of initial EDA). Percentage corresponds to distribution of products (diethyl fumarate and maleate accounted for 100% of initial EDA). TON values: 25 for [Cu], 30 for [Ag].

Scheme 6. Scale-up Functionalization of C–H Bonds with EDA and Complex 4 as the Catalyst

bonds of unreactive alkanes, we focused our attention on the improvement of the TON values. Cyclohexane and hexane were chosen as representative examples. Under similar conditions to those already described, 50 equiv of EDA with respect to the catalyst was added in one portion to a solution of complex 4 in neat alkane (see Experimental Section). At variance with the previous experiments, for which no EDA was detected after

3 h of stirring at room temperature, these reactions required higher reaction times (5–8 h). After that time no EDA was left in the reaction mixture, and conversions and selectivities were nearly identical to those in Schemes 3 and 4. Scale-up experiments were then carried out with 100 and 200 equiv of EDA relative to 4, again added in one portion. Surprisingly, no reaction was observed for 24 h (Scheme 6). When the experi-

ment with 200 equiv was performed using a syringe pump, however (EDA was slowly added over the course of 3 h into the flask containing the catalyst and the alkane, see Experimental Section), the reaction took place instantaneously. At the end of the reaction (3 h) no EDA was detected by GC, and 80–90% isolated yields of the expected products were obtained. Therefore, these experiments with the silver complex **4** as the catalyst have allowed the enhancement of the catalytic activity up to a TON value of 200 in 3 h with a catalyst loading of 0.5%. This represents a 10-fold increase in the TON value compared to any other coinage metal-based catalyst reported so far for this transformation, already in the range of some of the (less active) rhodium catalysts (see Table 1). We have no explanation as yet for the inhibition of the reaction at large EDA concentrations. Mechanistic studies are needed to clarify the importance of the catalyst:EDA ratio that ensures the catalytic transformation under certain conditions.

Conclusion

The new perfluorinated ligand [F₂₁-Tp^{4Bo,3CF3}] as well as the complexes [F₂₁-Tp^{4Bo,3CF3}]M(L) (M = Cu, Ag; L = NCMe, Me₂CO, CO) have been synthesized and fully characterized. The coinage metal complexes have been employed as catalysts for the decomposition of ethyl diazoacetate and the subsequent transfer of the CHCO₂Et unit to the C–H bonds of linear, branched, and cyclic alkanes. The activities shown by the silver derivative are remarkable, providing the highest TON values obtained to date for a group 11 metal-based catalysts for this transformation. Work aimed at improving activities and selectivities to the level of the most active catalysts is currently underway in our laboratories.

Experimental Section

All experiments requiring a dry atmosphere were performed using conventional vacuum line and Schlenk tube techniques or in a drybox. Acetonitrile, dichloromethane, and pentane were dried and distilled over CaH₂ under argon. Acetone was dried and stored over molecular sieves under argon. Ethyl diazoacetate, copper(I) iodide, and silver(I) triflate were purchased from Aldrich and used as received. Alkanes were dried with sodium and distilled. 3-Trifluoromethyl-4,5,6,7-tetrafluoroindazole was synthesized as previously described.¹¹ NMR solvents were stored over molecular sieves under argon. NMR data were recorded at 298 K using ARX-250, DPX-300, AV-500, or AV-600 MHz Bruker spectrometers or Varian Mercury 400. ¹⁹F NMR chemical shifts were referenced relative to an external CFCl₃ standard. Elemental analyses were performed in the Analytical Service of our laboratories. Mass spectroscopic data were recorded on a QTRAP Applied Biosystems mass spectrometer. IR spectra were recorded on a Perkin-Elmer 100, Perkin-Elmer GX, or Varian Scimitar. GC data were collected on Varian 3900 and 3800 instruments.

Synthesis of K[F₂₁-Tp^{4Bo,3CF3}]. KBH₄ was dried for 1 h under vacuum at 130 °C. KBH₄ (0.16 g, 3.0 mmol) and 3-trifluoromethyl-4,5,6,7-tetrafluoroindazole (2.50 g, 9.7 mmol) were introduced in a Schenk tube. The mixture was heated to 160 °C for 1 h. The yellow residue was washed three times with a pentane/toluene (2:1) mixture. K[F₂₁-Tp^{4Bo,3CF3}] was obtained as a white powder (1.02 g, 1.24 mmol, 41%). ¹⁹F NMR (282.40 MHz; acetone-*d*₆): δ –167.13 (pt, *J* = 18.9 Hz, 1F, F-5), –161.41 (pt, *J* = 18.9 Hz, 1F,

F-7), –155.74 (pt, *J* = 18.9, 10.0 Hz, 1F, F-6), –147.52 (qd, *J* = 13.8, 18.9 Hz, 1F, F-4), –61.13 (d, ⁵*J* = 13.8 Hz, 3F, CF₃). ¹¹B NMR (75.47 MHz, acetone-*d*₆): δ –0.47. ESI-MS: *m/z* (relative intensity) 783 (100, M⁺).

Synthesis of Tl[F₂₁-Tp^{4Bo,3CF3}] (1). A solution of thallium(I) sulfate (0.42 g, 0.83 mmol) in water (60 mL) was added to a solution of K[F₂₁-Tp^{4Bo,3CF3}] (1.025 g, 1.25 mmol) in chloroform (70 mL). The mixture was stirred for 4 h. The organic layer was then decanted, and the water extracted with chloroform (2 × 10 mL). After evaporation of the organic volatiles, a white powder was obtained that was recrystallized from dichloromethane to give colorless crystals of Tl[F₂₁-Tp^{4Bo,3CF3}] (**1**) (0.800 g, 0.81 mmol) in 65% yield. Single crystals were grown from slow evaporation of a dichloromethane solution. Anal. Calcd (%) for C₂₄HBF₂₁TlN₆: C 29.19, H 0.10, N 8.51. Found: C 29.06, H 0, N 8.59. ¹⁹F and ¹¹B NMR as for the K⁺ salt. ¹³C{¹H} NMR (62.90 MHz; CDCl₃): δ 139.4 (ddd, *J* = 250.2, 15.2, 15.2 Hz, C-5), 137.2 (dddd, *J* = 250.2, 12.5, 4.2, 4.2 Hz, C-4), 135.5 (ddd, *J* = 244.0, 15.6, 15.6 Hz, C-6), 134.6 (dd, *J* = 253.0, 12.20 Hz, C-7), 132.9 (q, *J* = 39.0 Hz, C-3), 131.6 (m, C-7a), 121.6 (q, *J* = 267.3 Hz, CF₃), 108.3 (dd, *J* = 19.2, 4.1 Hz, C-3a). ESI-MS: *m/z* (relative intensity) 783 (100, M⁺), 205 (100, M⁺).

Synthesis of [F₂₁-Tp^{4Bo,3CF3}]Cu(CH₃CN) (2). Copper iodide (33 mg, 0.17 mmol) was added to a solution of **1** (170 mg, 0.17 mmol) in acetonitrile (10 mL). The mixture was stirred for 4 h, and the solvent was removed under reduced pressure. The residue was extracted into dichloromethane (10 mL) and filtered through Celite. Dichloromethane was then evaporated to leave [F₂₁-Tp^{4Bo,3CF3}]Cu(CH₃CN) (**2**) as a white powder (88%). ¹H NMR (600.13 MHz; CDCl₃): δ 2.43 (s, 3H, CH₃). ¹⁹F NMR (282.40 MHz; CDCl₃): δ –161.54 (pt, *J* = 19.1 Hz, 1F, F-5), –153.15 (pt, *J* = 18.4 Hz, 1F, F-7), –151.96 (m, 1F, F-6), –143.31 (psxtet, *J* = 18.4 Hz, 1F, F-4), –59.89 (d, *J* = 18.4 Hz, 3F, CF₃). ¹³C{¹H} NMR (150.90 MHz; CDCl₃): δ 141.2 (ddd, *J* = 253.5, 15.1, 15.1 Hz, C-5), 137.7 (dd, *J* = 255.0, 12.1 Hz, C-4), 136.5 (ddd, *J* = 249.0, 15.1, 15.1 Hz, C-6), 135.3 (q, *J* = 39.2 Hz, C-3), 134.5 (ddd, *J* = 247.5, 12.1, 4.5 Hz, C-7), 131.1 (m, C-7a), 120.2 (q, *J* = 270.1 Hz, CF₃), 114.2 (s, CN), 107.5 (d, *J* = 19.6 Hz, C-3a), 2.2 (s, CH₃). Anal. Calcd (%) for C₂₂H₄BCuF₂₁N₇: C 35.18, H 0.45, N 11.05. Found: C 35.04, H 0.22, N 11.36.

Synthesis of [F₂₁-Tp^{4Bo,3CF3}]Cu(CO) (3). CO gas (1 atm) was bubbled through a solution of **2** in dichloromethane at 0 °C for 2 h. Hexane was added, and the resulting mixture was kept at –25 °C under a CO atmosphere to give colorless crystals of [F₂₁-Tp^{4Bo,3CF3}]Cu(CO) (**3**) in quantitative yield. The NMR experiments were carried out in a J. Young NMR tube under CO pressure. ¹⁹F NMR (282.40 MHz; CDCl₃): δ –159.87 (pt, *J* = 18.8 Hz, 1F, F-5), –151.88 (pt, *J* = 18.5 Hz, 1F, F-7/6), –150.96 (pt, *J* = 18.2 Hz, 1F, F-6/7), –142.15 (ph, *J* = 19.0 Hz, 1F, F-4), –59.21 (d, ⁵*J*_{FF} = 18.9 Hz, 3F, CF₃). ¹³C{¹H} NMR (125.81 MHz; CDCl₃): δ 171.8 (br s, CuCO), 141.8 (ddd, *J* = 255.4, 15.1, 15.1 Hz, C-5), 137.7 (dd, *J* = 256.6, 11.5 Hz, C-4), 136.9 (ddd, *J* = 251.6, 15.1, 15.1 Hz, C-6), 136.2 (q, *J* = 41.0 Hz, C-3), 134.4 (ddd, *J* = 257.9, 13.8, 5.0 Hz, C-7), 131.2 (m, C-7a), 119.9 (q, *J* = 270.5 Hz, CF₃), 107.5 (d, *J* = 18.9 Hz, C-3a). IR (CH₂Cl₂, cm^{–1}): 2126 (νCO); (solid state, cm^{–1}): 2657 (νBH), 2132 (PCO). Anal. Calcd (%) for C₂₅HBCuF₂₁N₆O: C 34.33, H 0.12, N 9.61. Found: C 34.35, H 0, N 10.13.

Synthesis of [F₂₁-Tp^{4Bo,3CF3}]Ag(CH₃COCH₃) (4). In a glovebox, **1** (100 mg, 0.10 mmol) and silver(I) triflate (26 mg, 0.10 mmol) were mixed in a Schlenk tube covered with aluminum foil. Acetone (8 mL) was added and the mixture was stirred overnight. The solvent was removed under reduced pressure, and the residue was extracted into dichloromethane (10 mL). After filtration through Celite and evaporation of the volatiles, [F₂₁-Tp^{4Bo,3CF3}]-Ag(CH₃COCH₃) (**4**) was obtained as a white powder (73%). Colorless crystals were grown by slow evaporation of an acetone

(23) 591 structures with terminal metal carbonyl complexes with C–O distances between 1.06 and 1.075 Å were found in the Cambridge Crystallographic Data Base.

(24) Braga, A. A. C.; Maseras, F.; Urbano, J.; Caballero, A.; Díaz-Requejo, M. M.; Pérez, P. J. *Organometallics* **2006**, *25*, 5292.

Table 2. Crystal Data and Structure Refinement for **1**, **2**, **3**, and **5**

	1	2	3	5
empirical formula	C ₂₄ HBF ₂₁ N ₆ Tl	C ₂₆ H ₄ BCuF ₂₁ N ₇	C ₂₅ HBCuF ₂₁ N ₆ O	C ₂₅ HAgBF ₂₁ N ₆ O
molecular weight	987.50	887.71	874.67	919.00
temperature [K]	180	100	180	180
wavelength [Å]	0.71073	0.71073	0.71073	0.71073
cryst syst	triclinic	monoclinic	monoclinic	monoclinic
space group	<i>P</i> $\bar{1}$	<i>Cc</i>	<i>P2₁/n</i>	<i>P2₁/n</i>
<i>a</i> [Å]	9.6514(9)	17.9262(10)	9.4150(6)	9.3110(6)
<i>b</i> [Å]	18.1834(17)	17.6733(10)	11.6353(8)	11.5542(9)
<i>c</i> [Å]	18.2284(17)	9.2157(6)	28.0159(16)	27.9217(19)
α [deg]	64.197(10)	90	90	90
β [deg]	89.612(11)	95.485(3)	94.000(3)	94.789(6)
γ [deg]	74.763(11)	90	90	90
<i>V</i> [Å ³]	2757.4(5)	2906.3(3)	3061.6(3)	2993.4(4)
<i>Z</i>	4	4	4	4
density (calcd) [Mg m ⁻³]	2.379	2.029	1.898	2.039
<i>F</i> (000)	1848	1728	1696	1768
absorp coeff [mm ⁻¹]	6.032	0.923	0.876	0.840
absorp corr	semiempirical	semiempirical	semiempirical	semiempirical
max./min. transm	0.469/0.341	0.816/0.769	0.918/0.842	0.855/0.721
cryst size [mm]	0.175 × 0.125 × 0.125	0.30 × 0.23 × 0.23	0.2 × 0.12 × 0.09	0.4 × 0.25 × 0.18
no. of refls collected	25926	38225	24837	22695
no. of indep refls	9484 [R(int) = 0.0755]	6238 [R(int) = 0.0418]	5339 [R(int) = 0.0466]	6130 [R(int) = 0.0215]
no. of data/restraints/params	9484/8/955	6238/2/506	5339/0/496	6130/0/496
final <i>R</i> indices [<i>I</i> > 2σ(<i>I</i>)] ^{a,b}	<i>R</i> ₁ = 0.0557, <i>wR</i> ₂ = 0.1468	<i>R</i> ₁ = 0.0273, <i>wR</i> ₂ = 0.0615	<i>R</i> ₁ = 0.0456, <i>wR</i> ₂ = 0.1067	<i>R</i> ₁ = 0.0341, <i>wR</i> ₂ = 0.0796
<i>R</i> indices (all data) ^{a,b}	<i>R</i> ₁ = 0.0697, <i>wR</i> ₂ = 0.1561	<i>R</i> ₁ = 0.0351, <i>wR</i> ₂ = 0.0647	<i>R</i> ₁ = 0.0743, <i>wR</i> ₂ = 0.1161	<i>R</i> ₁ = 0.0458, <i>wR</i> ₂ = 0.0865
goodness-of-fit on <i>F</i> ^{2c}	1.017	1.002	1.053	1.109

^a $R_1(F) = \sum(|F_o| - |F_c|) / \sum |F_o|$ for the observed reflections [$F^2 > 2\sigma(F^2)$]. ^b $wR_2(F^2) = \{\sum[w(F_o^2 - F_c^2)^2] / \sum w(F_o^2)^2\}^{1/2}$. ^c $S = \{\sum[w(F_o^2 - F_c^2)^2] / (n - p)\}^{1/2}$ (*n* = number of reflections, *p* = number of parameters).

solution or from a dichloromethane/pentane solution at -25 °C. ¹H NMR (500.33 MHz; CDCl₃): δ 2.88 (s, CH₃). ¹⁹F NMR (282.40 MHz; CDCl₃): δ -161.76 (pt, *J* = 19.2 Hz, 1F, F-5), -153.41 (pt, *J* = 17.8 Hz, 1F, F-7), -151.37 (m, 1F, F-6), -144.10 (psexet, *J* = 16.0 Hz, 1F, F-4), -60.54 (d, *J* = 15.2 Hz, 3F, CF₃). ¹³C{¹H} NMR (125.81 MHz; CDCl₃): δ 213.2 (s, CO), 141.2 (ddd, *J* = 254.1, 15.1, 15.1 Hz, C-5), 137.5 (dd, *J* = 254.1, 12.0 Hz, C-4), 136.4 (ddd, *J* = 249.1, 15.1, 15.1 Hz, C-6), 135.5 (q, *J* = 37.7 Hz, C-3), 134.7 (ddd, *J* = 256.7, 13.8, 5.0 Hz, C-7), 132.0 (m, C-7a), 120.3 (q, *J* = 269.2 Hz, CF₃), 107.5 (d, *J* = 20.1 Hz, C-3a), 32.0 (s, CH₃). Anal. Calcd (%) for C₂₇H₇AgBF₂₁N₆O: C 34.17, H 0.74, N 8.86. Found: C 34.01, H 0.45, N 8.97.

Synthesis of [F₂₁-Tp^{4Bo,3CF3}]₂Ag(CO) (5). CO gas (1 atm) was bubbled through a solution of **4** in dichloromethane at 0 °C for 2 h. Hexane was added and the resulting mixture was kept at -25 °C under a CO atmosphere to give colorless crystals of [F₂₁-Tp^{4Bo,3CF3}]₂Ag(CO) (**5**) in quantitative yield. The NMR experiments were made in a J. Young NMR tube under CO pressure. ¹⁹F NMR (282.40 MHz; CDCl₃): δ -160.71 (pt, *J* = 19.2 Hz, 1F, F-5), -152.05 (pt, *J* = 17.4 Hz, 1F, F-7), -151.15 (m, 1F, F-6), -143.41 (psexet, *J* = 16.0 Hz, 1F, F-4), -60.28 (dd, *J* = 15.2, 2.8 Hz, 3F, CF₃). ¹³C{¹H} NMR (125.81 MHz; CDCl₃): δ 178.6 (s, CO), 141.5 (ddd, *J* = 255.4, 15.1, 15.1 Hz, C-5), 137.6 (dd, *J* = 255.0, 12.6 Hz, C-4), 136.6 (ddd, *J* = 250.4, 15.1, 15.1 Hz, C-6), 136.2 (q, *J* = 39.0 Hz, C-3), 134.6 (dd, *J* = 257.9, 12.6 Hz, C-7), 132.0 (m, C-7a), 120.1 (q, *J* = 270.5 Hz, CF₃), 107.5 (d, *J* = 18.9 Hz, C-3a). IR (CH₂Cl₂, cm⁻¹): 2167 (νCO); (solid state, cm⁻¹): 2618 (PBH), 2167 (PCO).

General Catalytic Experiment. The catalyst (complex **2** or **4**, 0.008 mmol) was dissolved in 5 mL of the corresponding substrate, and 0.2 (for **2**) to 0.24 (for **4**) mmol of EDA was added in one portion to the stirred mixture at room temperature. Additional 5 mL of methylene chloride was added with the copper catalyst to ensure solubilization. The flask was covered with aluminum foil, in the case of silver as the catalyst, to avoid exposure to light. After 3 h of stirring no EDA was detected by GC. The mixture was investigated by GC, the volatiles were removed under vacuum, and the residue was investigated by NMR. The products were identified by comparison with reported chromatographic and spectroscopic data.⁹ Conversions correspond to, at least, an average of two runs

and were determined in the following manner. After removal of volatiles (at 0 °C to avoid loss of low boiling point compounds), the crude product was investigated by ¹H NMR spectroscopy, with a standard being added (tosyl chloride, styrene) to ensure that all the initial EDA was converted in the observed products. The observed ratios were compared to those from GC analysis at the end of the reaction, in order to establish the response factors. The subsequent experiments were then checked by GC using such factors.

The preparative experiments were run using 0.008 mmol of **4**, which was dissolved in 7 mL of the alkane. EDA was dissolved in 10 mL of the same alkane and slowly added for 3 h from a syringe pump. At the end of the reaction, the volatiles were removed at 0 °C and the product was separated by column chromatography. The alkanes employed were cyclohexane, hexane, and 2-methylpentane, with isolated yields of 80–90%.

X-ray Crystallographic Studies. Crystal data and structure refinement for complexes **1**, **2**, **3**, and **5** are given in Table 2, crystals being obtained as shown above. The selected crystals were mounted on a glass fiber using perfluoropolyether oil and fixed by rapid cooling in a stream of cold nitrogen. For all the structures data were collected at low temperature on a STOE IPDS diffractometer (**1**), a Bruker Kappa APEX II (**2** and **3**), equipped with an Oxford Cryosystems Cryostream cooler device, or an Oxford Diffraction Xcalibur diffractometer (**5**) equipped with a cryojet from Oxford Instrument, and using graphite-monochromated Mo K α radiation (λ = 0.71073 Å). Final unit cell parameters were obtained by means of a least-squares refinement of a set of 8000 well-measured reflections, and crystal decay was monitored during data collection by measuring 200 reflections by image; no significant fluctuation of intensities has been observed. Structures have been solved by means of direct methods using the program SIR92^{25a} or SIR2002^{25b} and subsequent difference Fourier maps. Models were refined by least-squares procedures on *F*² by using SHELXL-97²⁶ integrated

(25) (a) Altomare, A.; Cascarano, G.; Giacovazzo, G.; Guagliardi, A.; Burla, M. C.; Polidori, G.; Camalli, M. *J. Appl. Crystallogr.* **1994**, *27*, 435. (b) Burla, M. C.; Camalli, M.; Carozzini, B.; Cascarano, G. L.; Giacovazzo, C.; Polidori, G.; Spagna, R. SIR2002: the program. *J. Appl. Crystallogr.* **2003**, *36*, 1103.

in the package WINGX version 1.64²⁷ or in the Bruker software package,²⁸ and empirical absorption corrections were applied to all data.²⁹ All hydrogens atoms were geometrically placed and refined by using a riding model. All non-hydrogens atoms were anisotropically refined, and in the last cycles of the refinement, a weighting scheme was used, where weights are calculated from the following formula: $w = 1/[\sigma^2(F_o^2) + (aP)^2 + bP]$ where $P = (F_o^2 + 2F_c^2)/3$. For complexes **3** and **5**, it was not possible to properly resolve diffuse electron-density residuals (crystallization solvent molecules). Treatment with the SQUEEZE facility from PLATON³⁰ resulted in a smooth refinement. Since a few low-order reflections are missing from the data set, the electron count is

underestimated. Consequently, the values given for r_{calc} , $F(000)$, and the molecular weight are valid only for the ordered part of the structure.

Acknowledgment. We thank the MEC for financial support (CTQ2005-00324), the ERA Chemistry Programme, and the Junta de Andalucía (P07-FQM-2870). A.C. thanks the MEC for a research fellowship (Ramón y Cajal Program).

Supporting Information Available: Cif files and X-ray data for compounds **1–5**. This material is available free of charge via the Internet at <http://pubs.acs.org>.

OM800531A

(26) Sheldrick, G. M. *SHELX97*. [includes *SHELXS97*, *SHELXL97*, *CIFTAB*], Programs for Crystal Structure Analysis (Release 97-2); Institut für Anorganische Chemie der Universität: Göttingen, Germany, 1998.

(27) Farrugia, L. J. *J. Appl. Crystallogr.* **1999**, *32*, 837.

(28) Bruker, *Apex 2*, version 2.1; Bruker AXS Inc.: Madison, WI, 2004.

(29) Blessing, R. H. *MULTI SCAN*. *Acta Crystallogr.* **1995**, *A51*, 33.

(30) Spek, A. L. *Acta Crystallogr.* **1990**, *A46*, C-34.